Open Access Journal
Journal of Power Technologies 94 (4) (2014) 259–269
journal homepage:papers.itc.pw.edu.pl

Greening the future of transport by using a regenerative variable geometry gas turbine engine

Yousef S. H. Najjar*,[a], Hussein N. Dalgamoni[b]

[a]Jordan University of Science and Technology
Ar Ramtha, Irbid 22110, Jordan
[b]University of Tabuk
Tabuk 71491, Saudi Arabia

Abstract

Gas turbine engines are cleaner, have multi-fuel capability, and a lower volume to power ratio than piston engines. A main disadvantage of gas turbine engines in automotive use is their poor part-load efficiency. As transport engines spend most of their operating life at part-load; a gas turbine engine that achieves a wide range of high-efficiency should be used. This paper aims to develop a computer model to simulate the performance of regenerative gas turbine engines for transport use. A computer program for the performance prediction was designed based on the characteristics of each component in the engine and the compatibility between them. The influence of a variable power turbine setting-angle on engine performance was investigated. Compressor and turbines maps were used in a particular form; hence, each point on the map has a specific value of rotational speed, pressure ratio, mass flow rate, and efficiency. Variation in effectiveness of the regenerator was considered. Variable pressure drop and mass flow rate across the combustion chamber and the regenerator were included.

Keywords: Regenerative gas turbines, Variable geometry power turbine, Modeling, Simulation, Transport, Green technology

1. Introduction

The trend for increasingly stringent global regulation of pollutant emissions and vehicle fuel efficiency has spurred researchers to look for new alternatives to replace or at least to play down the use of conventional piston engines. One of these proposed alternatives is the transport gas turbine engine. Projects are now directed toward improving the vehicle's power, reducing exhaust emissions, and improving fuel economy by using gas turbine engines in transport. To improve fuel efficiency, at part-load, a regenerative engine with variable power turbine geometry presents the simplest turbine cycle capable of competing with piston engines [1]. This enables the gas entering the turbine to do so at an elevated temperature, therefore increasing efficiency and reducing fuel consumption.

Cycle variables and components characteristics are essential in engine performance models [2]. Whalley and Ebrahimi [3] investigated a multivariable model of an automotive gas turbine. Juhasz [4] generated an open cycle gas turbine numerical modeling code suitable for thermodynamic performance analysis of automotive and aircraft power plant appli-

*Corresponding author
Email addresses: y_najjar@hotmail.com (Yousef S. H. Najjar*), hussein412@yahoo.com (Hussein N. Dalgamoni)

cations. Lazzaretto and Toffolo [5] represented a gas turbine model, at design and off-design conditions, through an appropriate scaling technique of a generalized compressor and turbine maps taken from literature and validating them with test measurement data.

Campanari [6] investigated the thermodynamic potential of integrating solid oxide fuel cell technology and microturbine systems, in order to obtain a high-efficiency, small capacity power plant. Campanari described the procedure to model microturbine engines with and without an integrated solid oxide fuel cell.

Kim et al. [7] investigated comparatively off-design steady-state performance and operating characteristics of single and two-shaft gas turbines for electric generation. They derived a set of equations based on the validated component models. A simultaneous calculation schematic was employed that was flexible in respect of various engine configurations.

Kim and Hwang [8] analyzed the performance characteristics of a recuperated gas turbine at part-load conditions. They considered various part-load operation strategies including simple (fuel only control), variable speed, and variable inlet guide vane operations for single-shaft configuration as well as simple and variable area nozzle (VAN) operations for the two-shaft configuration. They concluded that the variable speed operation of the single-shaft configuration provides the most efficient part-load operation.

McLallin and Kofskey [9] experimentally determined the cold-air performance of the baseline power turbine designed for a 112-kilowatt automotive gas-turbine engine. They presented the overall performance in terms of mass flow, torque, speed, and efficiency at variable setting angles of the power turbine stator. They concluded that turbine efficiency varied significantly with stator setting angle. Turbine mass-flow and torque levels increased as the setting angle increased.

Most of the previous models were for simple gas turbine engines or lacked the ability to deal with large variations in operating parameters. In this study, the performance analysis was done based on mass flow, rotational speed, and power compatibility between components over a wide range of operating parameters. Compressor and turbine characteristics were provided in a particular form; hence, each point on the map has specific values of rotational speed, pressure ratio, mass flow rate, and efficiency. Variable pressure drop in the combustion chamber and regenerator was applied. Variations in specific heats, regenerator effectiveness, and leakage flow were considered.

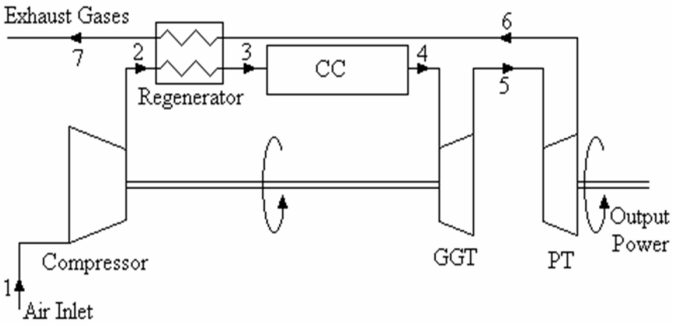

Figure 1: Schematic diagram of regenerated free PT gas turbine engine

2. Regenerative Gas Turbine (RGT)

Fig. 1 represents a schematic diagram of a regenerative free PT gas turbine engine. The major components are: compressor, regenerator, combustion chamber (CC), gas generator turbine (GGT), and free power turbine (PT). The compressor is a single stage, centrifugal type, with a pressure ratio of 4.2 at design point. The regenerator, which is a rotary moving element heat exchanger, is made up of highly porous discs of either a stainless steel or a ceramic construction. The gas turbines used are two single-stage axial turbines [10–12]. The GGT produces power to drive the compressor and the engine accessories, while the PT, located downstream of the GGT, is mounted on an independent shaft, and connected to the load.

3. Design Point Performance

Performance prediction requires finding the corresponding operating points on the characteristics map of each component when the engine is running at a steady-speed, or in equilibrium. When these equilibrium-running points are obtained they may be plotted on the compressor map and joined up to form an equilibrium-running line.

Table 1: Compressor DP performance data

Inlet temperature T_{01}, K	288
Inlet pressure P_{01}, kPa	101
Inlet mass flow rate $\dot{m}_C = \dot{m}_1 = \dot{m}_2$, kg/sec	1.07
Pressure ratio PR_C	4.20
Isentropic efficiency η_C, %	82.0
Power input PW_C, kW	193

Table 2: CC DP performance data

CC efficiency, %	90.0
Relative pressure drop $\Delta P_{0,CC}/P_{03}^2$, %	2.50

Design point performance data for the compressor, CC, GGT, regenerator, and PT, are presented in Tables 1–5.

4. Off-Design Performance

4.1. Implementation of components

To predict the off-design performance of gas turbine engine, the components' characteristics are needed. The compressor map [6] was reproduced using Smooth C software as shown in Fig. 2. Fig. 2a shows the efficiency contours and Fig. 2b shows the β-lines. For each speed line with a fixed β-line one can obtain consistent value of PR_C, $\dot{m}_C\sqrt{T_{01}}/P_{01}$, and η_C. The compressor map was tabulated in array form, as shown by Fig. 3, and entered into the computer model.

GGT and PT maps [9, 13] were reproduced using Smooth T software. Fig. 4 represents GGT map, Fig. 5, 6, 7 and 8 represent PT map at 26°, 30°, 35° (DP), and 45° SA. Fig. 9 shows turbine maps in array form; these arrays were entered into the computer model.

Table 3: GGT DP performance data

Inlet temperature T_{04}, K	1260
Inlet pressure P_{04}, kPa	398
Pressure ratio PR_{GGT}	1.90
Mass flow rate $\dot{m}_{GGT} = \dot{m}_4 = \dot{m}_5$, kg/sec	1.00
Isentropic efficiency η_{GGT}, %	86.0
Power output PW_{GGT}, kW	195

Table 4: PT DP performance data

Inlet temperature T_{05}, K	1100
Inlet pressure P_{05}, kPa	209
Pressure ratio PR_{PT}	1.66
Mass flow rate $\dot{m}_{PT} = \dot{m}_5 = \dot{m}_6$, kg/sec	1.00
Isentropic efficiency η_{PT}, %	74.2
Power output PW_{PT}, kW	113
Setting-angle, °	35.0

Table 5: Regenerator DP data

	Air-side	Gas-side
Inlet temperature T_{06}, K	466	1010
Inlet pressure P_{06}, kPa	426	127
Relative pressure drop $\Delta P/P_{inlet}$, %	4.00	13.5
Leakage mass flow rate percentage (seal and carryover), %	–	+7.50
	7.50	
Effectiveness $\varepsilon_{reg,DP}$, %	90.0	

In the combustion chamber a constant value of efficiency was used (i.e. 99%) and a variable value of pressure drop was modeled by Equation (1).

$$\frac{\Delta P_{0,CC}}{P_{03}} = \left(\frac{\Delta P_{0,CC}}{P_{03}}\right)_{DP}\left(\frac{\left(\frac{\dot{m}_3\sqrt{T_{03}}}{P_{03}}\right)}{\left(\frac{\dot{m}_3\sqrt{T_{03}}}{P_{03}}\right)_{DP}}\right)^2 \quad (1)$$

The term 'performance of the regenerators' includes three main items namely, effectiveness of heat transfer, pressure drop, and leakage performance or the mass loss percentage. Approximate off-design regenerator effectiveness can be modeled as [14, 15]:

$$\varepsilon_{reg} = 1 - \left(\frac{\dot{m}_2}{\dot{m}_{2,DP}} \times \left(1 - \varepsilon_{reg,DP}\right)\right) \quad (2)$$

Off-design air-side local pressure drop in regenerator can be approximated as [15]:

$$\frac{\Delta P_{reg,a}}{P_{02}} = \left(\frac{\Delta P_{reg,a}}{P_{02}}\right)_{DP} \times \left(\left(\frac{\dot{m}_2}{P_{02}}\right)^2\left(\frac{T_{03}^{1.55}}{T_{02}^{0.55}}\right) / \left(\frac{\dot{m}_2}{P_{02}}\right)_{DP}^2\left(\frac{T_{03}^{1.55}}{T_{02}^{0.55}}\right)_{DP}^2\right) \quad (3)$$

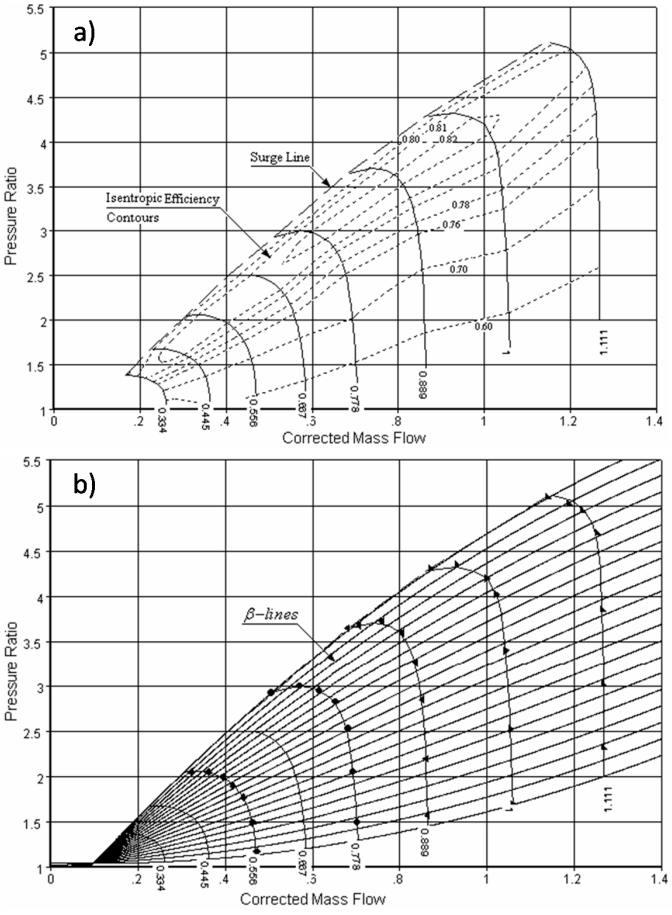

Figure 2: Compressor map with isentropic efficiency contours (a), compressor map with β-lines (b)

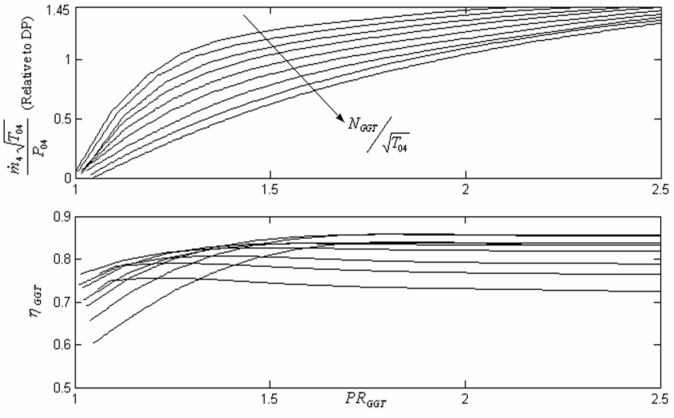

Figure 4: GTT map

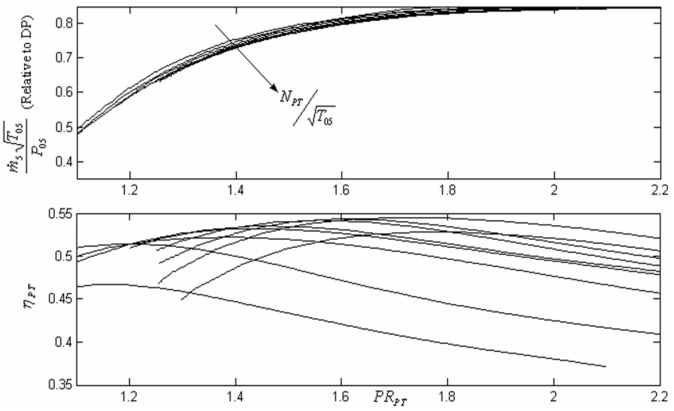

Figure 5: PT map at 26° setting-angle

In addition, off-design gas-side pressure drop in the regenerator can be approximated as [15]:

$$\frac{\Delta P_{reg,g}}{P_{06}} = \left(\frac{\Delta P_{reg,g}}{P_{06}}\right)_{DP} \left(\frac{\dot{m}_6^2 \times T_{06}}{\left(\dot{m}_6^2 \times T_{06}\right)_{DP}}\right) \qquad (4)$$

Leakage performance, or the mass loss percentage, includes the carry-over loss associated with the void volume of the matrix. Carryover leakage presents quite a small fraction of the compressor flow, usually less than 1% of the compressor flow [15]. Another type of mass loss in the regenerator is seal leakage; this type of leakage is much greater than the carry-over leakage and represents the dominant mass loss in the regenerator. Seal leakage can be as much as 10% of the mass flow rate leaving the compressor. In a well-designed regenerator, seal leakage can be reduced to a value of approximately 5%. Both seal and carry-over leakages were considered as a fixed percentage of 7.5% of the compressor discharge mass flow rate at the DP ($\dot{m}_{2,DP}$) and all off-design conditions [14, 15].

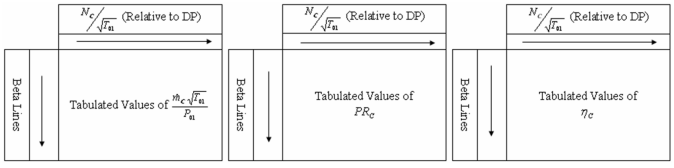

Figure 3: Compressor map representation in array form

The average value of specific heat at constant pressure during compression or expansion was approximated using equation (5) [16].

$$\bar{C}_{P,AB} = 950 + 0.21 T_{0A} \qquad (5)$$

The value of specific heat ratios for air and gas was considered constant, i.e. $\gamma_a = 1.4$ $\gamma_g = 1.33$.

The elements that contribute to the total power requirement of an automotive are aerodynamic drag,

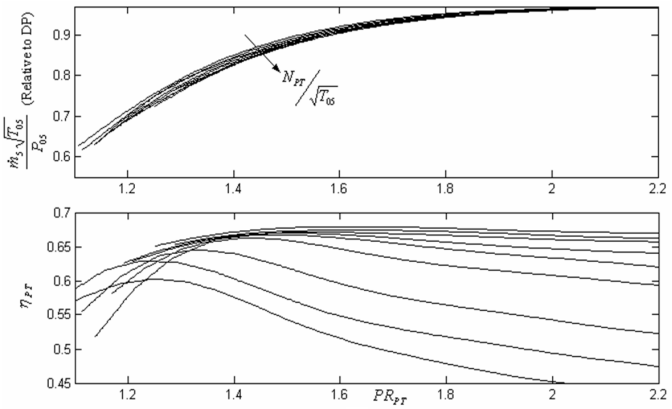

Figure 6: PT map at 30° setting-angle

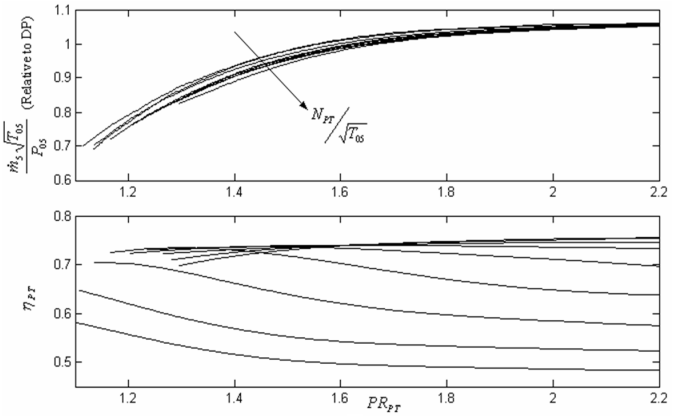

Figure 7: PT map at 35° setting-angle (DP)

rolling resistance, hill climb, and acceleration. The total power required to maintain vehicle velocity and acceleration could be calculated as:

$$PW_{LOAD} = F_{LOAD} \times V_{Vehcile} \tag{6}$$

Where ($V_{Vehcile}$) is vehicle velocity, and (F_{LOAD}) is the total propulsive force to maintain vehicle velocity and acceleration. (F_{LOAD}) can be calculated as;

$$F_{LOAD} = F_{Drag} + F_{Roll} + F_{C\ell imb} + F_{Accel} \tag{7}$$

Where (F_{Drag}) is drag force, (F_{Roll}) rolling resistance force, ($F_{C\ell imb}$) hill climbing force, and (F_{Accel}) is acceleration force. A relation between the total propulsive power required by the load and the power turbine speed can be obtained by expanding equation (7) and substituting in equation (6) as:

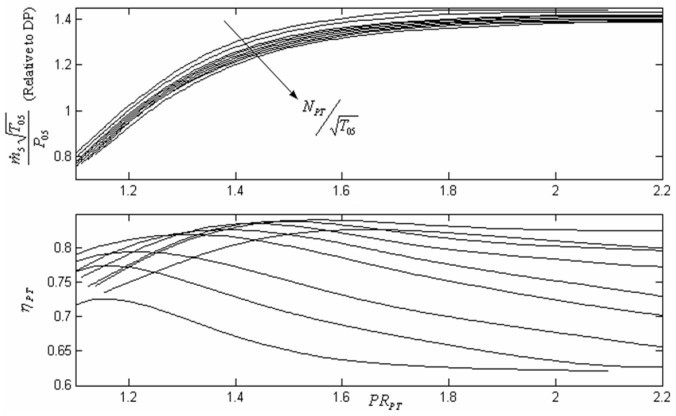

Figure 8: PT map at 45° setting-angle

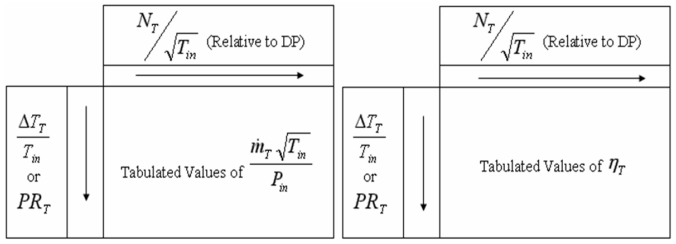

Figure 9: Turbine map representation in arrays form

$$\begin{aligned} PW_{LOAD} &= \left(F_{Drag} + F_{Roll} + F_{C\lim b} + F_{Accel}\right) \times V_{Vehcile} \\ &= \left\{\left[\frac{\rho_{air}}{2}\left(V_{Wind} + \left\{\frac{2\pi}{60}\frac{N_{PT}}{GR}Rad_{Wheel}\right\}\right)^2 Cd\, A_{Front,Vehcile}\right] \right. \\ &\quad + \left[C_{Roll}\, m_{Vehicle}\, g\right] + \left[\sin(Ang_{C\lim b})\, m_{Vehicle} g\right] \\ &\quad \left. + \left[m_{Vehicle}\, Accel\right]\right\} \times \left\{\frac{2\pi}{60}\frac{N_{PT}}{GR}Rad_{Wheel}\right\} \end{aligned} \tag{8}$$

When the vehicle specifications, environmental and operational conditions are known, the load characteristic in terms of the net power actually required by the load versus the PT speed can be plotted.

Fig. 10 represents a load characteristics curve for a typical family saloon car, using cube law (propeller law).

4.2. Matching of Components

The 'Match Point' is defined as the steady-state operating point for a gas turbine engine when the compressor and turbine are balanced in rotor speed, power, and mass flow rate [11, 17]. Off-design operation can be estimated according to the fulfillment of rotational speed, mass flow rate, and power compatibility between components.

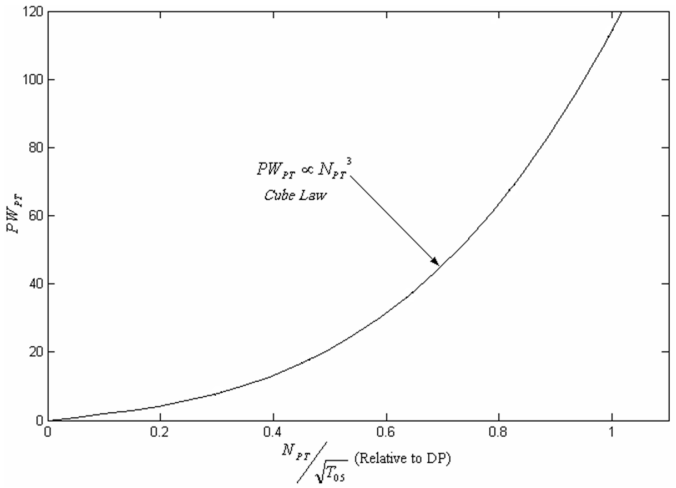

Figure 10: Load characteristics

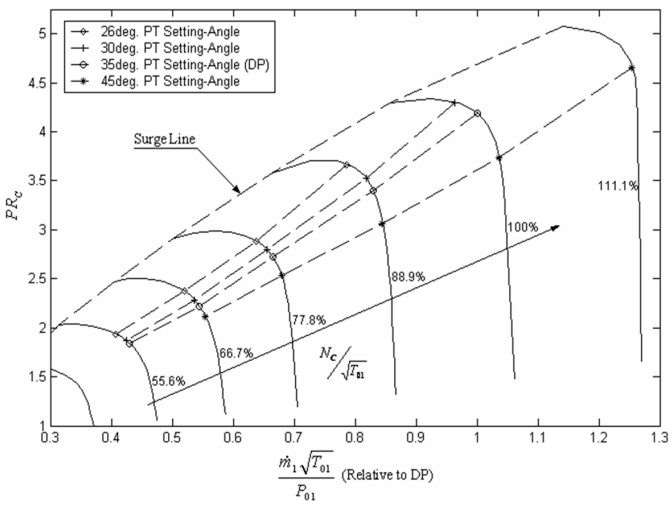

Figure 12: Engine equilibrium-running lines at various PTSA

In a gas turbine engine with a free PT, the compressor is directly coupled to the GGT; this requires three constraints:

1) The rotational speed of compressor equals the rotational speed of GGT,

$$\frac{N_C}{\sqrt{T_{01}}} = \frac{N_{GGT}}{\sqrt{T_{04}}} \times \sqrt{\frac{T_{04}}{T_{01}}} \tag{9}$$

2) The mass flow rate entering the GGT equals the mass flow rate at the compressor delivery minus the mass flow rate losses in the regenerator plus the mass flow rate of fuel,

$$\frac{\dot{m}_4\sqrt{T_{04}}}{P_{04}} = \frac{\dot{m}_1\sqrt{T_{01}}}{P_{01}} \times \frac{1}{PR_C} \times \frac{1}{\left(1-\frac{\Delta P_{reg,a}}{P_{02}}\right)} \times \frac{1}{\left(1-\frac{\Delta P_{CC}}{P_{03}}\right)} \times \sqrt{\frac{T_{04}}{T_{01}}} \times \frac{\dot{m}_4}{\dot{m}_1} \tag{10}$$

3) GGT must deliver the power required to drive the compressor.

$$\dot{m}_1 \bar{C}_{P,12} \frac{T_{01}}{\eta_C}\left(PR_c^{\frac{\gamma_C-1}{\gamma_C}} - 1\right) = \eta_{mech}\dot{m}_4 \bar{C}_{P,45} T_{04} \eta_{GGT}\left[1 - \left(\frac{1}{PR_{GGT}}\right)^{\frac{\gamma_{GGT}-1}{\gamma_{GGT}}}\right] \tag{11}$$

The PT matched to the GGT by the compatibility of the mass flow rate passes them, i.e. the mass flow rate passes the PT, equals the mass flow rate, passes the GGT, and it depends on the swallowing capacity of the PT.

$$\frac{\dot{m}_5\sqrt{T_{05}}}{P_{05}} = \frac{\dot{m}_4\sqrt{T_{04}}}{P_{04}} \times PR_{GGT} \times \sqrt{\frac{T_{05}}{T_{04}}} \tag{12}$$

The PT, which is coupled to the load, should match the power required by the load characteristics

$$PW_{PT} = PW_{LOAD}\,. \tag{13}$$

It is important to consider the characteristics of the load to determine whether the compressor operating point represents a valid solution; in the case of automotive applications, the power needed by the load varies with the cube of the rotational speed of the power turbine. When the transmission efficiency, gear ratio and other factors were known, the load characteristic can be represented in terms of PT output power and speed as shown in Fig. 10.

Predicting the performance of a gas turbine engine is a highly iterative procedure. Iteration continues until the balance in speed, power, and mass flow rate between components is satisfied. Once the iteration is completed, the cycle parameters can be derived; Fig. 11 represents the flowchart of the iteration procedure.

5. Results and discussion

A computer model was developed to simulate the performance of a regenerative automotive gas turbine engine. The model satisfies the compatibility of mass flow rate, rotational speed, and power output between the engine components. The effect of VPTSA on engine performance was investigated.

Fig. 12 represents the engine equilibrium-running lines at different PTSA plotted on the compressor map. When PTSA is increased, the running line moves away from the compressor surge line, and

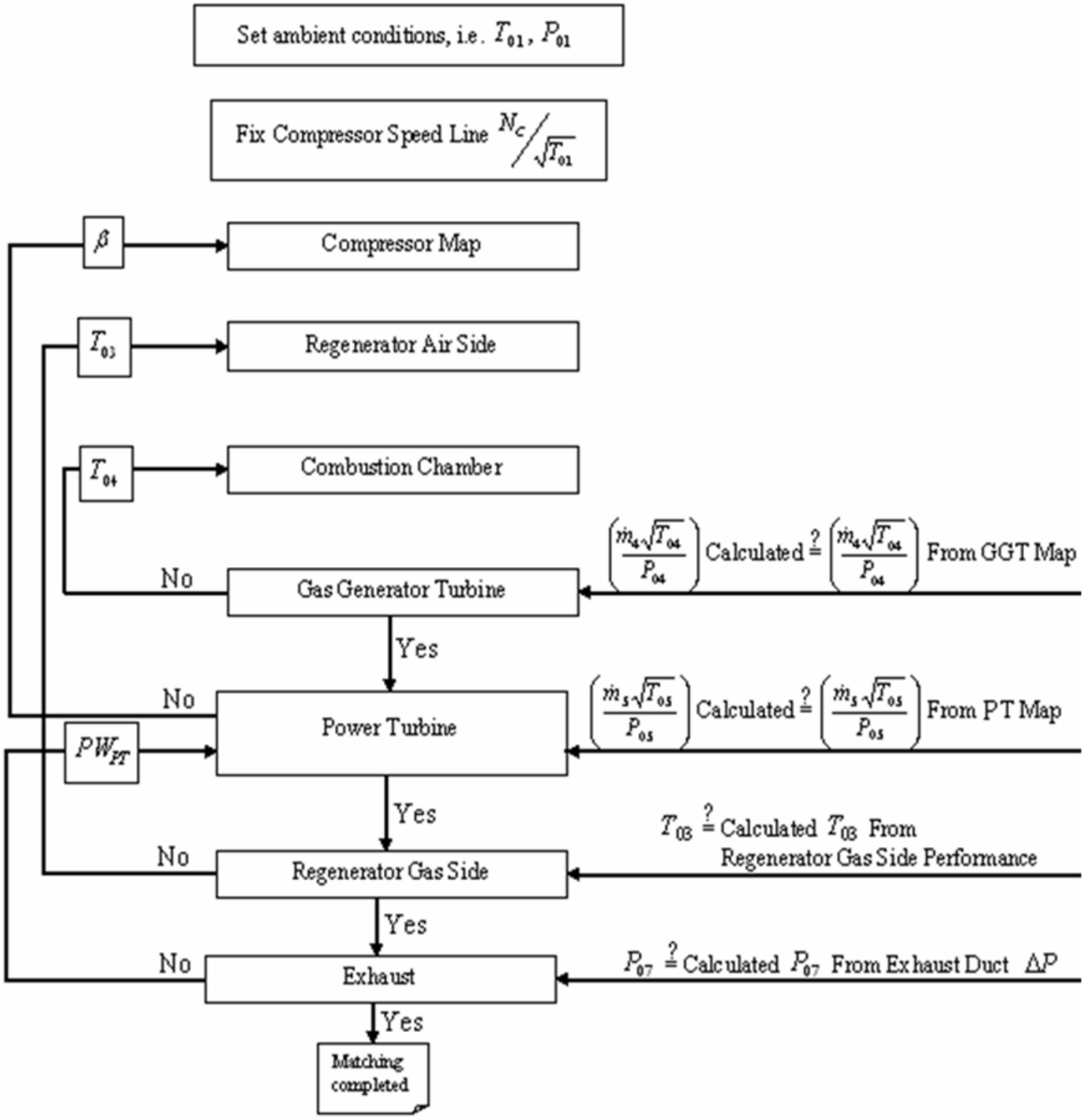

Figure 11: Model flowchart

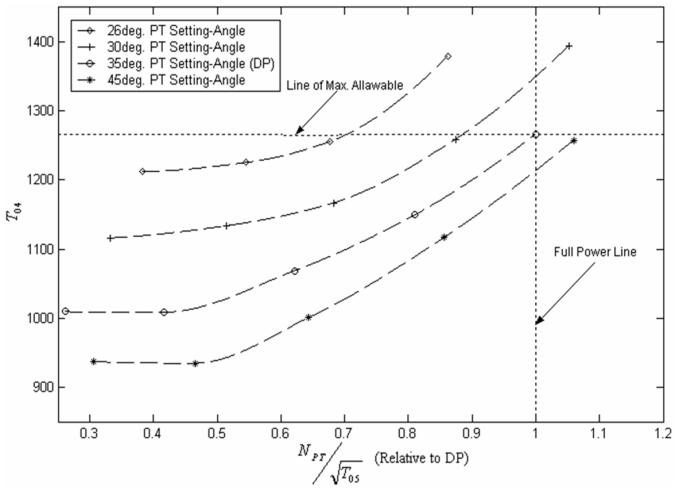

Figure 13: GGT inlet temperature versus PT speed at various PTSA

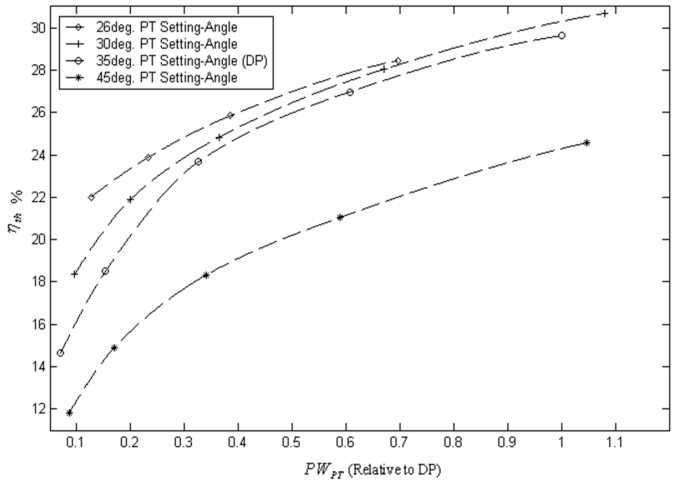

Figure 14: Engine thermal efficiency versus output power at various PTSA

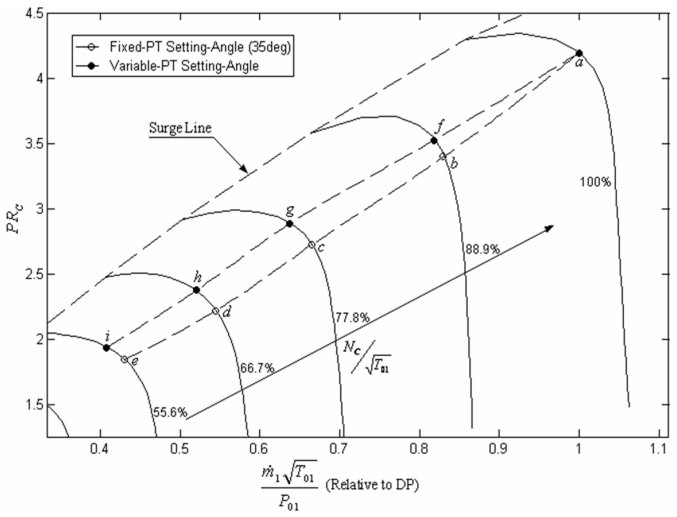

Figure 15: Engine running lines with F/VPTSA

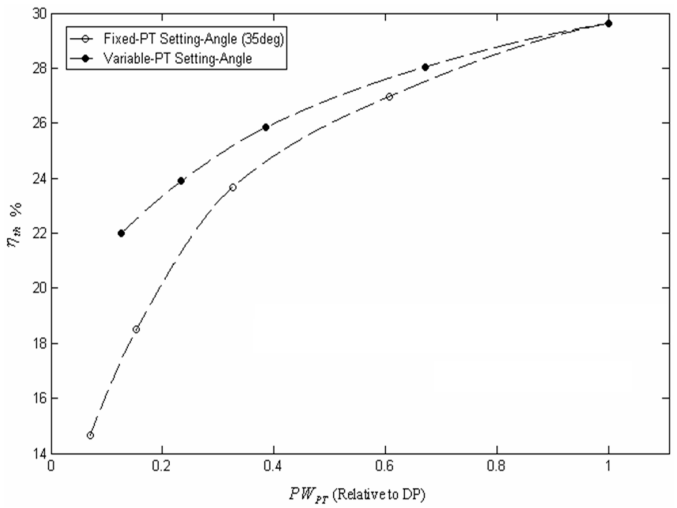

Figure 16: Engine thermal efficiency versus engine output power with F/VPTSA

when PTSA is reduced the running line moves toward the compressor surge line, the last trend increases GGT inlet temperature, as shown in Fig. 13.

In Fig. 13 at 26° and 30°, the maximum allowable GGT inlet temperature is attained at PT speeds equal to 70% and 88% of the DP speed; this mean that the engine cannot be brought to its full power at those values of PTSA.

Fig. 14 shows thermal efficiency as $\eta_{th}\frac{PW_{PT}}{\dot{m}_f \Delta H_{25}\eta_{CC}}$ at different values of PTSA. Higher values of thermal efficiency are achieved at lower PTSA. Furthermore, the drop in thermal efficiency is less significant at lower PTSA; this implies that a further reduction in the engine output power requires a reduction in PTSA in order to keep engine thermal efficiency as high as possible.

The engine equilibrium-running line with VPTSA can be plotted on a compressor map by connecting the equilibrium-points that represent maximum thermal efficiency. Fig. 15 shows the equilibrium-running line of the engine with FPTSA and with VPTSA; the later tracks closer to the compressor surge line. This running line represents the best/lowest bsfc for the engine over its operating range.

Fig. 16 shows the thermal efficiency of the engine versus power output. The thermal efficiency of the engine is always higher, especially at part-load when VPTSA is used. Table 6 represents the gain in ther-

Table 6: Engine thermal efficiency

Engine output power, %	Engine thermal efficiency FPTSA, %	VPTSA, %	Gain in thermal efficiency, %
100	29.6	29.6	0.00
67.0	27.5	28.1	0.60
38.5	24.6	25.8	1.20
23.3	21.3	23.9	2.60
12.7	17.4	22.0	4.60

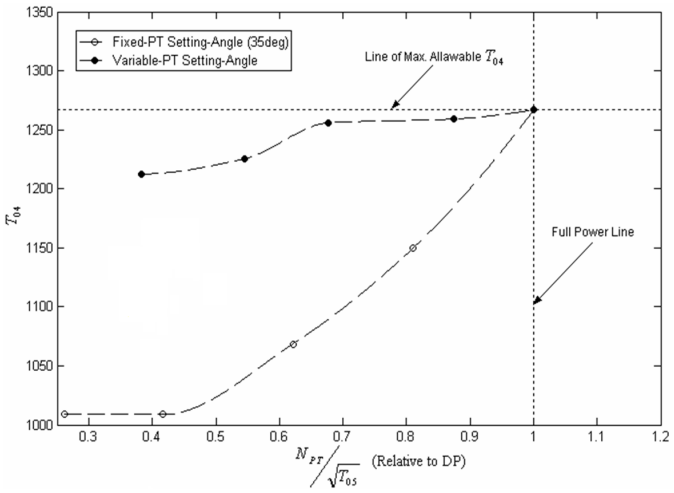

Figure 17: GGT inlet temperature versus PT speed with FVPTSA

mal efficiency when using VPTSA; i.e. at a power output of 38.5%, reducing PTSA from 35° to 26° causes a 14% increase in GGT inlet temperature, hence the thermal efficiency of the engine increases by 1.2%.

When using VPTSA the values of GGT inlet temperature are always above 97% of its DP value even at extreme part-load operation, see Fig. 17. Fig. 18 represents the output power of the engine versus GGT speed with F/VPTSA. The same output power engine is attained at a lower value of GGT speed when VPTSA is used.

6. Conclusions

Gas turbine engine performance modeling requires knowledge of the characteristics of components in a particular arrangement. Engine performance characteristics at part-load depend on a combination of factors. The basic improvement in the engine part-load performance results from maintaining high GGT inlet temperature at part-load, which can be controlled by reducing/increasing PTSA and this will improve engine part-load performance. Each PTSA yields unique PT characteristics; which results in a unique equilibrium-running line and unique performance curves.

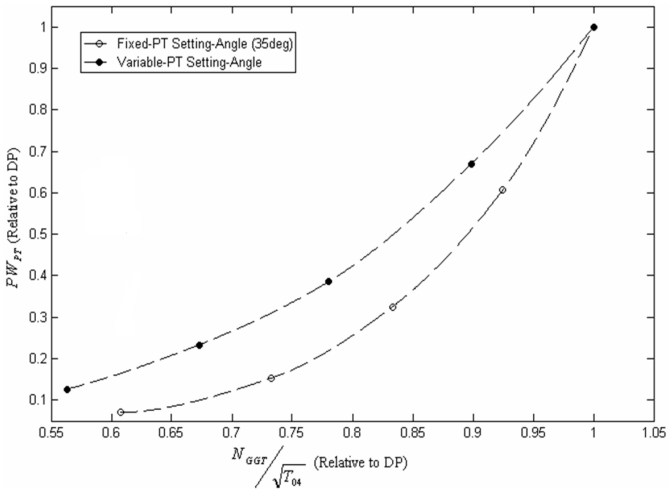

Figure 18: Engine output power versus GGT speed with F/VPTSA

GGT inlet temperature increases with the reduction in PTSA. That is at reduced values of PTSA, the GGT inlet temperature exceeds its maximum allowable value. As a result, this means that the engine cannot be brought to its full power at that PTSA.

VPTSA is essential in improving part-load thermal efficiency in automotive applications. With VPTSA, the gain in thermal efficiency can reach 4.6% over that for FPTSA at extreme part-load operation of 12.7% of the design point power output.

References

[1] D. Barbeau, The Performance of Vehicle Gas Turbines. SAE Technical Paper 670198 (1967). doi:10.4271/670198.

[2] D. Wilson, K. Theodosios, Models for predicting the performance of brayton-cycle engines, Engineering for Gas Turbines and Power 116 (1994) 381–388.

[3] R. Whalley, M. Ebrahimi, Automotive gas turbine regulation, IEEE transaction on Control Systems Technology 12 (3) (2004) 465–473.

[4] A. Juhasz, Automotive gas turbine power system-performance analysis code, NASA Technical Memorandum 107386 (1997) 1–5.
[5] A. Lazzaretto, A. Toffolo, Analytical and neural network models for gas turbine design and off-design simulation, Applied Thermodynamics 4 (4) (2001) 173–182.
[6] S. Companari, Full load and part-load performance prediction for integrated sofc and microturbine systems, Engineering for Gas Turbines and Power 121 (2000) 239–246.
[7] J. Kim, T. Kim, J. Sohn, S. Ro, Comparative analysis of off-design performance characteristics of single and two-shaft industrial gas turbines, Engineering for Gas Turbines and Power 125 (2003) 954–960.
[8] T. Kim, S. Hwang, Part load performance analysis of recuperated gas turbines considering engine configuration and operation strategy, Energy 31 (2006) 260–277.
[9] K. McLallin, M. Kofskey, Cold-air performance of free power turbine designed for 112-kilo Watt automotive gas-turbine engine, Tech. rep., USA DOE/NASA (February 1979).
[10] D. Wilson, K. Theodosios, The Design of High-Efficiency Turbomachinery and Gas Turbines, 2nd Edition, Prentice-Hall Inc, New Jersey, 1998.
[11] W. Bathie, Fundamentals of Gas Turbines, 2nd Edition, John Wiley and Sons Inc, New York, 1996.
[12] H. Saravanamuttoo, G. Rogers, H. Cohen, Gas Turbine Theory, 5th Edition, Pearson Education Limited, London, 2001.
[13] J. Horlock, Axial Flow Turbines, Butterworths, London, 1966.
[14] W. Kays, A. London, Compact Heat Exchangers, 3rd Edition, McGraw-Hill Company, New York, 1984.
[15] P. Walsh, P. Fletcher, Gas Turbine Performance, 2nd Edition, Blackwell Science and ASME, New Jersey, 2004.
[16] R. Harman, Gas Turbine Engineering, Macmillan Press LTD, London, 1981.
[17] F. Haglind, Variable geometry gas turbines for improving the part load performance of marine combined cycles-combined cycle performance, Applied Thermal Engineering 31 (2011) 467–476.

Nomenclature

ΔH_{25}	Enthalpy of Reaction, kJ/kg
Δ	Delta, the Difference
η	Isentropic Efficiency
η_{CC}	Efficiency of Combustion
η_{mech}	Mechanical Efficiency
η_{th}	Thermal Efficiency
γ	Specific Heats Ratio
ρ	Density, kg/m^3
ε	Effectiveness
$bsfc$	Brake Specific Fuel Consumption, kg/kJ
C_P	Specific Heat at Constant Pressure, kJ/(kg·K)
fa	Fuel Air Ratio
m	Mass, kg
N	Rotational Speed, rad/s
P	Pressure, kPa
PR	Pressure Ratio
PW	Power, kW
R	Gas Constant, kJ/(kg·K)
T	Temperature, K
x_{reg}	Mass Leak Percentage in the Regenerator
$bsfc$	brake specific fuel consumption
CC	combustion chamber
DP	design point
FSA	fixed setting-angle
PT	power turbine
PTSA	power turbine setting-angle
SA	setting-angle
VSA	variable setting-angle
1 2 3 4 5 6 7	State Conditions
a	air
atm	atmospheric
C	compressor
CC	combustion chamber

DP	design point
$Exhaust$	exhaust duct
f	fuel
GGT	gas generator turbine
$leak$	leakage
$LOAD$	load
min	minimum
PT	power turbine
ref	reference value
reg	regenerator
s	isentropic
0	Stagnation
$-$	Average
$\bullet$	Rate
$^\circ$	Degree